# A Case Study of Deformation Measurements of Istanbul Land Walls via Terrestrial Laser Scanning

Maryna Batur, Onur Yilmaz, and Haluk Ozener

***Abstract*—Historical structures, buildings, bridges, and walls are very sensitive to deformations which can be caused by many factors, such as winds, heavy rains, extreme temperature variations, ground and soil settlements, tectonic loadings, and others. The mapping of 3-D deformation maps of building provides an opportunity not only to understand the structural changes, but also to detect zones with a potential risk of damage. The high spatial resolution of terrestrial laser scanning (TLS) technology allows monitoring historical buildings with millimeter accuracy. Two towers of Istanbul Land Walls were surveyed three times with the 5-month time interval. The accurate deviation maps were obtained from TLS's data by comparing epochs. Between first two campaigns, there happened an earthquake with the magnitude of Mw 5.7 with the epicenter of approximately 60 km from the study area. The findings and outputs of this article indicate that earthquake had a great impact on the monitored structures and deformations were found up to 15 mm for the tower I and up to 20 mm for the tower II.**

***Index Terms*—Cultural heritage, displacement, geodetic monitoring, Istanbul Land Walls, point cloud, terrestrial laser scanning (TLS).**

## I. Introduction

HISTORICAL sites and structures play a very important role in the life of modern humanity because they reflect the history and culture of the nations. It is a core issue that concerns preservation and maintaining of the heritages for our descendants. During their long life, historical buildings suffer from many factors—weaknesses in foundations, movements in soil, chemical reactions, thermal changes, tectonic loadings etc., and they force the structure to undergo internal stresses that result in horizontal and vertical displacements. Geodetic monitoring allows to determine these displacements and, thus, provides the current structural state of the building and may predict its future behavior. There are many different techniques as well as their combinations that can be used for geodetic monitoring of historical structures. For example, the application of Total Station instrument for heritage monitoring is shown in [1]. Authors conducted five campaigns of measurements and compared them. The results did not show any vertical or horizontal movement of the structure and additional survey using terrestrial laser scanning (TLS) technology was done. After comparing two different scans, the previous results were verified that there were not any displacements. In [2], a group of Gothic buildings in Valencia that have a historical value were monitoring by leveling. As a result, significant displacements were observed in places where structural weaknesses were most expected. Another deformation study of historical building is shown in [3]. The historical Bell Tower in Italy was taken under the geodetic monitoring due to weak settlement foundation and earthquake risk. The structure was monitored by two techniques—leveling and TLS. Results obtained from TLS validated the previous findings from leveling and settlements were found as 0.5 mm per year. In [4], authors performed the damage assessment of historical temple that tilted due to ground subsidence. Two 3-D models of studied structure were created: the first model was based on Laser Imaging Detection and Ranging data (LiDAR) and the second model was generated from uncalibrated images. Using these models, the angles of inclinations were estimated. In [5], two case studies based on the use of 2-D and 3-D LiDARs showed that LiDAR allows the extraction of accurate building features and accomplishes in monitoring and analysis of relevant areas. The combination of TLS and photogrammetry for structural monitoring are shown in [6]. The aim of the article was to analyze the stability of historical Olympic Theatre in Vicenza (Italy) by applying finite-element model analysis to 3-D models derived from TLS and photogrammetry data. In [7], there is an example of InSAR application for the deformation monitoring of cultural heritage site. The Summer Palace (Beijing) was chosen as a case study. The results from high-resolution SAR images showed that studied site underwent deformations in some areas where, as authors state, the impact of urbanizations led to the subsidence. Related literature about the building detection using InSAR can be found in [8], where satellite data were applied to monitor ground deformations in landslides areas. First, authors used data recorded by C- and X-band satellites to obtain a displacement time-series of the area in Moio della Givitella (Italy). Then, in order to assess the structural performance of buildings located in this area, authors used a numerical code on computational model. Another application of Differential SAR Interferometry (DInSAR) technique is shown in [9]. The authors proposed a DInSAR workflow for dam monitoring, which was validated with *in situ* measurements. The methodology was applied for two case studies—Campolattaro Dam and Campotosto Dam and presented results validate the proposed methodological approach emphasizing the advantages of the current methodology. In [10], 61 COSMO-SkyMed images were processed to generate a displacement time series. Selected study area is Palma Campania

Manuscript received August 27, 2020; revised September 30, 2020; accepted October 13, 2020. Date of publication October 21, 2020; date of current version November 2, 2020. This work is supported by SRP Grant NO. 16764 (Bogazici University Scientific Research Project BAP project code: 20TP4). *(Corresponding Author: Maryna Batur)*

The authors are with the Department of Geodesy, Boğaziçi University, Istanbul 34342, Turkey (e-mail: maryna.batur@boun.edu.tr; onur.yilmaz@boun.edu.tr; ozener@boun.edu.tr).

Digital Object Identifier 10.1109/JSTARS.2020.3031675

town which covers about 20 $km^2$. Additionally, *in situ* survey was implemented to achieve a building assessment. As a result, most of the buildings showed very low displacements rated less than 2 mm per year, while some of buildings showed displacements about 4 mm per year and only one structure was exposed to 8 mm per year displacements. In [11], the ancient Church in Italy was chosen to investigate deformations due to earthquake that occurred between the two measurement campaigns via TLS. Deviation maps that were obtained from point cloud data showed clear structural changes. In [12], three cases were presented on the study of damages buildings by TLS. The first study concerned the historical Sivillier Castle. The Digital Surface Model was created from the point cloud data which then was used to analyze structural changes. The aim of the second study was to detect displacements from vertical axis of Bell Tower. The third and the last case concerned the investigation of industrial building that was partially damaged by the fire. Using 3-D model, damaged part and details of the structure were easily detected and geometrically identified. The interesting method of estimation the deformations in heritage structure by TLS was presented in [13]. The column of an ancient Temple in Greece, which was built in 330 B.C., was chosen for the study. First, the mesh surface was derived from the scanned data. After that, the column was divided into 13 drums and each part was analyzed separately. The center and the radius of each drum were calculated using known mathematical equations. This data were compared with the initial positions which were known from the previous surveys. As a result, column was found to move from its preliminary position on 66 mm. Similar research is shown in [14], where the 386 years old historical mosque in Istanbul was chosen for the study due to the inclination of its minaret. The minaret was divided into 31 sections and for each section inclination values were calculated. As a result, the total tilt was found to be 4063 cm. An interesting study is shown in [15], where three different quality assessment approaches were compared in terms of time and cost. These approaches are conventional approach with Total Station, TLS-based approach with manual data analysis, and TLS-based approach with automated data analysis. The construction site of a pet farm in Singapore was chosen for the case study. As the result, in terms of time, automated data analysis using TLS had a high time efficiency, while approach with manual data analysis was found as the most cost-efficient.

It appears from the above that conventional geodetic techniques, such as Total Station or leveling give good results in monitoring the displacements, but they are narrowed to the study of individually selected points and sometimes do not give an opportunity to investigate the whole object. TLS technology, in its turn, allows to record data on a large scale of measurements and in a short period of time and certainly gives advantages over other surveying methods. TLS technology also proved to be more effective compare to close-range photogrammetry [16]. There are various studies that take benefits of TLS on documentation and modeling heritages such as Diyarbakir Walls in Turkey [17], tower of Belem in Lisbon [18], and Umayyad Palaces in Jordan [19].

The objective of this article is to examine the two towers of the Land Walls of Istanbul for the displacements due to massive cracks on the front side of the structure by using TLS technology. The importance of this article is that the study area is located in Istanbul, which is part of the UNESCO World Heritage Site, and this area has never been studied before in terms of deformations. Besides, the second significant contribution of the article is that the site is prone to expected Istanbul earthquake, thus, the creation of an archive of the buildings in a digital environment is significant in order to prepare the base for the relief and restoration works. During the processing, three TLS campaign of measurements were performed in order to compare the point cloud data from different epochs using cloud-to-cloud (C2C) method of distance computation [20], [21] and a rapid knowledge of the structural state of the investigated object was obtained.

## II. Historical Background of Studied Structure and Aim of the Study

The Walls of Istanbul, also known as the Walls of Constantinople and Theodosian Walls, is the most important historical structure of the city, their construction dates back to 413 A.D. Controlled by Roman, Byzantine, Latin, and Ottoman Empires, Walls had mainly defensive purposes, but also surveyed as a border of city. The Walls of Istanbul consisted of three parts: Land Walls, Sea Walls, and Golden Horn Walls, which can be seen in Fig. 1(a). The very little part of it survived hitherto. Historical Land Walls consisted of moat, low, outer, and inner walls. Moat wall is over 20 m wide and 10 m deep, is fenced with low wall and served as the first line of defense. Today, this area is used for the gardening purposes. The outer wall was built between the low and inner walls and was used as the second line of defense. This part was 2 m thick with the height of 9 m. The main and the most important part of Land Walls is the inner wall with 5 m thick and 12 m high. Both the outer and inner walls are strengthened with towers that are spaced at average distance of approximately 40–60 m. Only a small part of outer walls and their towers have survived until today. The towers of inner wall have squared form with size 10 by 10 m and the height of 20 m and were made of limestone bricks [22]. The map, construction scheme of Land Walls, and their current state are shown in the Fig. 1(a)–(c).

To examine two towers of the Land Walls [see Fig. 1(d) and (e)], initially, it was of interest to perform the geodetic monitoring based on two campaign of measurements, however, due to earthquake that occurred between the first two epochs with the magnitude of Mw 5.7 and with the epicenter of approximately 60 km from the studied area, it was decided to perform a third measurement and compare the results in order to see if there is an impact of earthquake. The workflow of the research is shown in Fig. 2.

To validate these assumptions, we used the following hypothesis:

Hypothesis $H_0$ (Null hypothesis): $D_1 = D_2$—the value of displacements computed in the first and the second periods, respectively, are identical. There is no impact of earthquake on the structure.

Hypothesis $H_1$ (Alternative hypothesis): $D_1 \neq D_2$—the value of displacements computed in the first and the second periods,

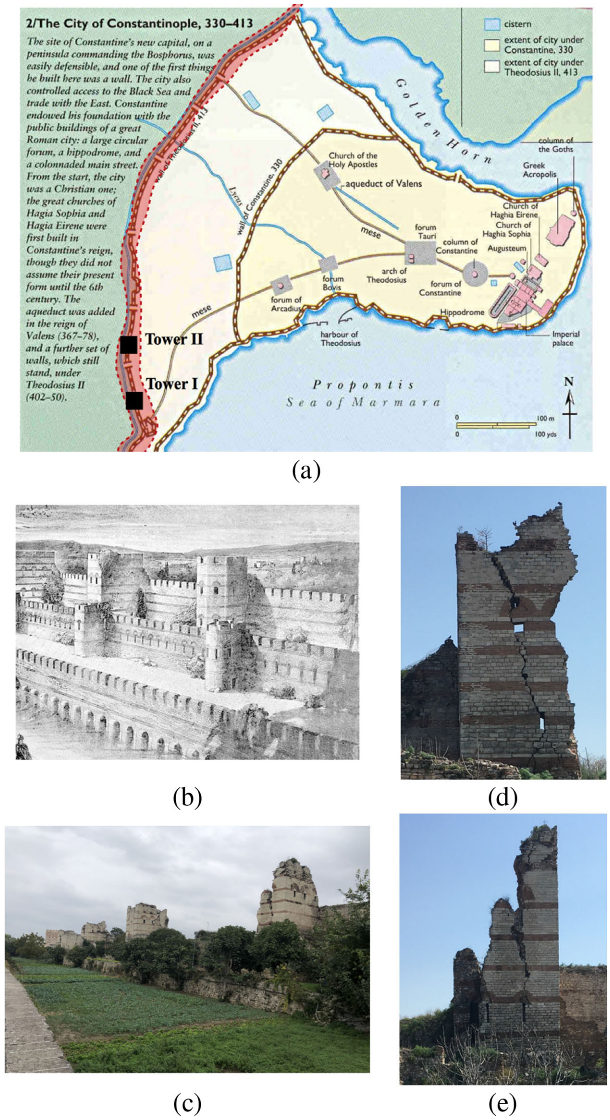


Fig. 1. Case study area. (a) Old map of Historical Peninsula of Istanbul showing Land Walls by red color [23]. (b) Sections of the Land Walls [22]. (c) Current state of Land Walls. (d) Studied tower I. (e) Studied tower II.

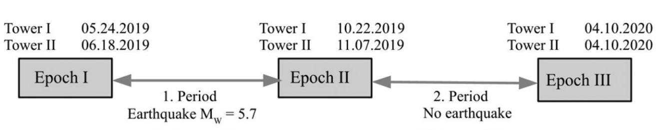


Fig. 2. Workflow of geodetic monitoring.

respectively, are not identical. In this instance, the following two cases have place.

1) $D_1 > D_2$—the displacements of the structure directly relevant to the earthquake.
2) $D_1 < D_2$—most probably there is other reason for displacements regardless of earthquake.

The most interesting aspect of our article is that this investigation deals not only with current time displacements, but also with displacements occurred throughout centuries, because

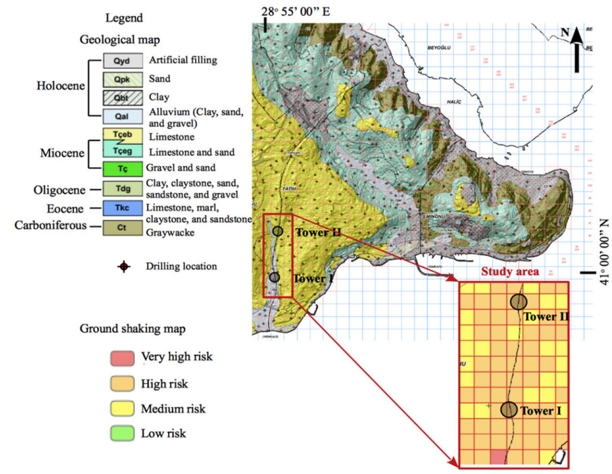


Fig. 3. Geological map and the ground shaking map of Historical Peninsula showing study area by red rectangle [33].

there has not been any restoration works in this part of Land Walls [24]. Another important fact is that, as we know, there has never been carried out a research on displacement measurements in this area. Some of the previous works were focused on the study of geology and microzonation of this area [25]–[27]. The authors of [28] conducted the geotechnical study of Land Walls and proposed a methodology that may prevent a collapse of the towers. In [29], the digital recording of the Land Walls was done using TLS and Photogrammetry methods. In addition, this structure is a part of Historic Areas of Istanbul and since 1985 it has been included in the UNESCO World Heritage Site. Istanbul Land Walls are of great historical value and there is a need to monitor this structure for the future maintaining and reconstruction.

## III. Geological Settings and Seismicity of the Case Study Area

Being the most historically and culturally important area of Istanbul, Historical Peninsula was repeatedly studied on its geological conditions. For example, in [30], geological and geotechnical findings from 125 drillings were used to obtain a detailed geological map of Historical Peninsula. The study area was divided into 250 $\times$ 250 m sections, and for each section a soil amplification map was obtained. Another study [31] was aimed to investigate the relationship between human activities and ground deformations based on DInSAR measurements in the area of Historical Peninsula of Istanbul. Results from that research allowed to detect potentially risky areas. In [32] and [27], the geological characteristics of Istanbul are discussed, and a detailed geological map of Istanbul city is presented.

Municipal Council of Istanbul is also conducted several studies concerning Istanbul microzonation maps.

According to Fig. 3, the Land Walls' territory is geologically characterized by the presence of Miocene formations, which is mainly made up of limestones, sands, and gravels. The ground shaking map shows that studied towers lay in the area of high risk from a certain probability of occurring an earthquake.

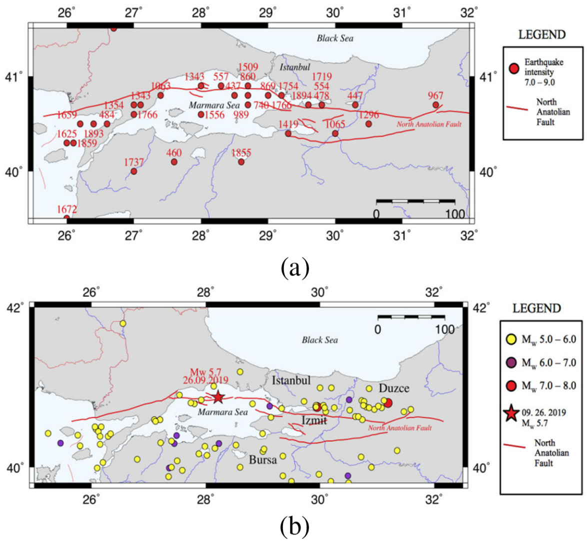


Fig. 4. (a) Historical earthquakes of Marmara region in the period of 400–1900 years given by [36] and [37]. (b) Historical earthquakes of Marmara region in the period of 1900–2019 years given by [38].

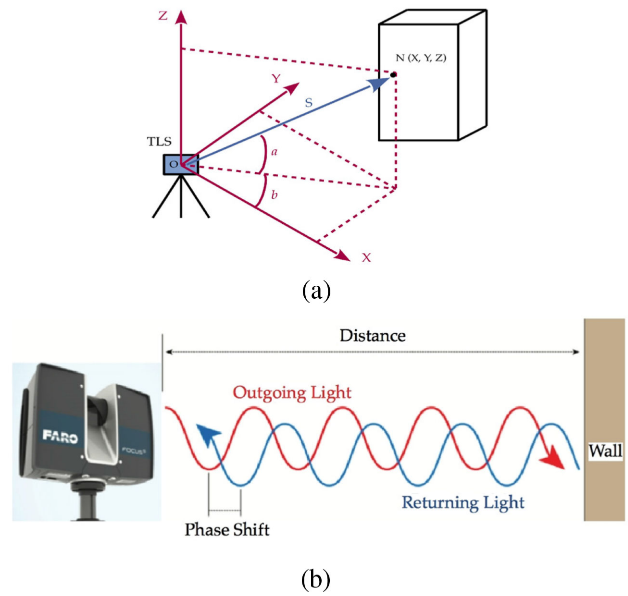


Fig. 5. (a) Principle of measurements in TLS FARO Focus 330 HDR. (b) Phase-shift distance determination [41].

The Land Walls are located near the Marmara Sea region, which is considered to be one of the most seismically dangerous zones in Turkey. The North Anatolian Fault, that runs through the basin of the Marmara Sea, produced many earthquakes in the past and as many different scientific studies show that the risk of new event is still very high [34], [35]. According to earthquake catalog of "KOERI-Regional Earthquake Tsunami Monitoring Center," in each historical period, Land Walls overcame many strong earthquakes such as 447, 554, 740, 989, 1509, 1766, 1754, 1894, and 1999 [36]–[38]. After some major and destructive earthquakes, some parts of the Land Walls were razed, and the reinforcement of these Walls was impossible to be applied. Thus, the Land Walls were reconstructed repeatedly.

Istanbul–Silivri earthquakes occurred on September 24 and 26, 2019. On 24th September 2019 at 09:00 UTC (11:00 local time), the medium intensity earthquake (Mw= 4.5) occurred in the Marmara Sea near Silivri. Two days after the previous earthquake, on September 26, 2019 at 11:59 UTC (13:59 local time), medium intensity earthquake (Mw= 5.7) occurred in the Marmara Sea at the 10 km depth in Istanbul–Silivri. Both medium earthquakes' epicenters were approximately 60 km from the Land Walls. Fig. 4(a) shows the earthquakes happened in the historical period 400–1900 years and Fig. 4(b) shows the epicenters of earthquakes occurred in the instrumental period 1900–2020 years, including earthquake that struck last time.

## IV. Materials and Methods

Structure to be surveyed as well as its surroundings are what dictates the choice of proper survey methodology and instruments. In our article, we preferred TLS technology because it provides 3-D perspective that allows for detailed survey and does not require direct physical contact with the structure.

The FARO Focus 330 HDR was used to scan the structure with further data processing in SCENE software, which is the manufacturer's software. A number of studies were performed using TLS FARO with further data processing in SCENE [17], [18], [39], [40] and they proved that FARO is one of the most successful instruments for scanning the historical buildings. Besides, its portability and compactness greatly facilitate the process of survey. In this respect, in our article, we used TLS FARO Focus 330 HDR. This instrument scans objects up to 330 m away covering 360° of horizontal and 300° of vertical field of view. According to its technical specifications, FARO Focus 330 HDR has a ranging error ±2 mm at around 10 m and allow to measure up to 976 000 points per second [41].

The main principle of measurements in TLS FARO Focus 330 HDR is based on the sending the laser beam to the object of interest, which is reflected from the surface and turn to the instrument, thus, recording the distance from itself to the object. The direction of laser beam is determined by two angles—vertical a and horizontal b, which can be seen in Fig. 5(a). Distance, vertical, and horizontal angles make up Polar coordinates, which is then transformed into Cartesian coordinates by (1)

$$\begin{cases} X_N = S.\cos b.\cos a \\ Y_N = S.\sin b.\cos a \\ Z_N = S.\sin a \end{cases} \tag{1}$$

where

$X_N$, $Y_N$, $Z_N$ – Cartesian coordinates of point $N$;
$S$ – Length of laser beam emitted from TLS to the object;
$a$ – Angle between the $ON$ and the $XY$-plane; and
$b$ – Angle between $X$-axis and the projection of ON onto the $XY$-plane.

To measure the distance to the object, TLS FARO Focus 330 HDR uses phase-shift technology that is shown in Fig. 5(b). Unlike scanners based on time-to-flight principle, where distance

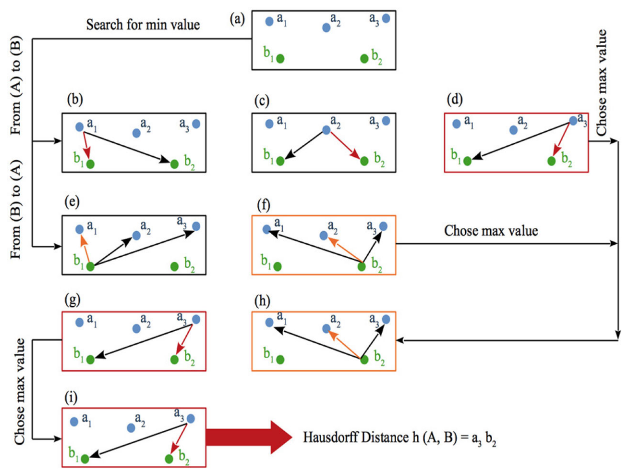


Fig. 6. Basic concepts of C2C distance computation method.

measurement consists of measuring the time between emitted and reflected laser pulse, the phase-based scanners measure the phase-shift of a pulse and distance to the object is calculated along sinusoidally modulated laser pulse. Several studies, for example, [42] and [43], have been carried out to compare these types of scanners and TLS based on phase-shift distance measurement proved to be better instrument for surveying.

To calculate displacements, C2C distance computation method was used. This method was developed based on the Hausdorff distance [44], which can be defined as a maximum distance of a set to the nearest point in the other set [45]

$$h\left(A_p, B_p\right) = \max_{a\epsilon A}\left\{\min_{b\epsilon B}\left\{d\left(a_A, b_B\right)\right\}\right\} \tag{2}$$

where

$a_A$ – points of set $A_p$;
$b_B$ – points of set $B_p$; and
$d\left(a_A, b_B\right)$ – Euclidean distance between $a_A$ and $b_B$.

Fig. 6 shows the basic concept of C2C distance computation method as follows.

1) There are two point cloud data sets $(A) = (a_1; a_2; a_3)$ and $(B) = (b_1; b_2)$; The algorythm first searches for minimum distance value from each point in (A) to every point in (B).
2) Minimum distance from $a_1$ to every point of (B) is $a_1b_1$.
3) Minimum distance from $a_2$ to every point of (B) is $a_2b_2$.
4) Minimum distance from $a_3$ to every point of (B) is $a_3b_2$.
5) Minimum distance from $b_1$ to every point of (A) is $b_1a_1$.
6) Minimum distance from $b_2$ to every point of (A) is $b_2a_2$. Then, the algorithm searches for maximum distance value among those minimum values that were found in previous steps.
7) Maximum distance among $a_1b_1$, $a_2b_2$, and $a_3b_2$ is $a_3b_2$.
8) Maximum distance among $b_1a_1$ and $b_2a_2$ is $b_2a_2$.
9) Maximum distance among $a_3b_2$ and $b_2a_2$ is $a_3b_2$ thai is the Hausdorff Distance.

The value of displacement is calculated for each point in dataset as a subtraction of reference coordinate from the measured in *X*, *Y*, and *Z* directions. The displacement vector, or 3-D displacement value, is then calculated according to (3)

$$3\mathrm{D}_{\mathrm{disp}} = \sqrt{\left(X_{\mathrm{meas}} - X_{\mathrm{ref}}\right)^2 + \left(Y_{\mathrm{meas}} - Y_{\mathrm{ref}}\right)^2 + \left(Z_{\mathrm{meas}} - Z_{\mathrm{ref}}\right)^2} \tag{3}$$

where:

$X_{\mathrm{meas}}, Y_{\mathrm{meas}}, Z_{\mathrm{meas}}$ – Planar coordinates of the compared frame;
$X_{\mathrm{ref}}, Y_{\mathrm{ref}}, Z_{\mathrm{ref}}$ – Planar coordinates of the reference frame.

Nowadays, there are plenty of software for the displacement analysis available for use [46]. One of them is Cyclone 3DR (previously termed Reshaper), which owned by Leica Geosystems Company and was used in different applications. For example, in [47], deviation analysis of tunnel was performed in this software package by comparing two different epochs using C2C distance computation method. Another study [48] presents the structural deformation analysis of historical church that was also done in this software. In [49], the deformation monitoring of historical Mihrimah Sultan Mosque (Turkey) was done in Cyclone 3DR. In our article, we used the demo version of Cyclone 3DR software for displacement computations.

## V. Data Acquisition and Processing

The methodology is organized according to the flowchart shown in Fig. 7.

The work begins with the site documentation, which provides insight into the work complexity and time required for a certain task. Based on the reconnaissance of the study area, the appropriate survey tools and the geometry of scanning can be selected. The geometry of scanning is determined by the TLS and target positions, which locations should be chosen to guarantee a maximum coverage of the scanned object without any obstructions in the line of sight. Once the scanning geometry is designed, the scanning parameters need to be specified. The next step is data processing, which consists of three steps: registration of scans, registration of epochs, and point cloud filtering. The last step is displacement computation, which is done by C2C method of distance computation.

### *A. Site Documentation and Field Operations*

Just before the data acquisition, the visual inspection of the study area and structures was done. Towers are located at the distance of approximately 1500 m, thus, each of towers was scanned separately. The surroundings of towers have the same geometrical features; therefore, the scanning configuration was similar for both towers. The acquisition of 3-D point clouds was carried out only in the western part of towers due to presence of huge cracks on this side. TLS was set up at three scan positions at a distance of 40 m from the structure, thus, getting the structure in maximal coverage. The distance between TLS positions was 20 m. In order to register scans together, spherical targets with a diameter of 145 mm were used. The main advantage of using these targets that they do not require direct physical contact with the object was important in our article. The configuration of targets is based on the scanning parameters with resolution and

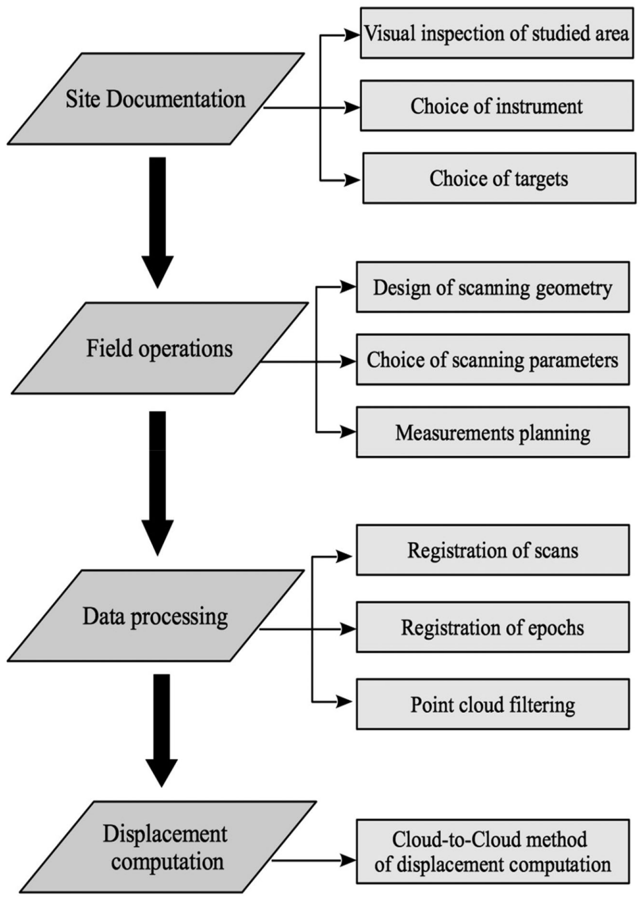


Fig. 7. Workflow of geodetic monitoring.

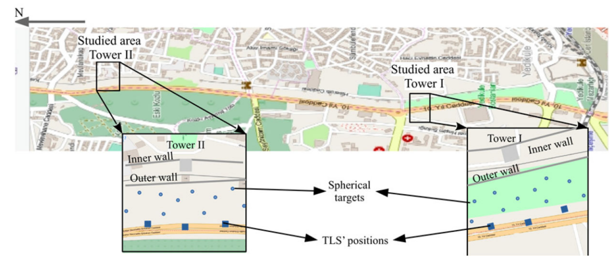


Fig. 8. Map showing the study area, TLS', and targets' positions.

TABLE I
SESSION PLANNING

| | Epoch I | Epoch II | Epoch III |
|---|---|---|---|
| Tower I | 05.24.2019 | 10.22.2019 | 04.10.2020 |
| Tower II | 06.08.2019 | 11.07.2019 | 04.10.2020 |

TABLE II
TARGET STATISTICS FOR THE TOWER I

| | Epoch I 05.24.2019 | Epoch II 10.22.2019 | Epoch III 04.10.2020 |
|---|---|---|---|
| Mean distance error, mm | 0.8 | 2.9 | 2.2 |
| Mean horizontal error, mm | 0.8 | 0.5 | 1.4 |
| Mean vertical error, mm | 0.1 | 2.8 | 1.4 |

TABLE III
TARGET STATISTICS FOR THE TOWER II

| | Epoch I 06.18.2019 | Epoch II 11.07.2019 | Epoch III 04.10.2020 |
|---|---|---|---|
| Mean distance error, mm | 2.1 | 2.0 | 2.6 |
| Mean horizontal error, mm | 1.1 | 1.0 | 1.5 |
| Mean vertical error, mm | 1.6 | 1.5 | 1.7 |

quality. Resolution determines the density of points, namely, distance between points. Quality, in its turn, determines how long the scanner takes to measure a point and the length of time a point is sampled. Quality affects the rate of measurements and the level of noise reduction. In our article, the scanning resolution was chosen as 1/1 meaning that the total number of scan points is 699.1 MPts with point distance of 1.5 mm on 10 m, and quality was chosen as 1x, which means that every point was fired one time by a laser beam. These settings are recommended by the manufacturers for displacement analysis study. We used the same resolution and quality settings for each TLS's position and during all epochs. It took approximately 20 min to scan the structure from each station that takes 1 h in total. The minimum and the maximum distances from TLS to the nearest target were 10 and 20 m, respectively. These distances were chosen according to [41] and based on the scanning parameters. Fig. 8 shows the configuration of scanning in relation to towers.

The data consisted of three epochs, which dates are shown in Table I.

## B. *Data Processing*

The point cloud processing was performed in SCENE software and proceeded in three stages as follows.

1) Registration of scans taken from different TLS' positions.
2) Registration of epochs for further displacement computation.
3) Point cloud filtering.

When object is scanned, points are tracked and recorded in the TLS's coordinate system. The number of these coordinate systems is equal to the number of TLS station points. In order to determine the spatial relation between all these scans, registration process is needed. This was done by target-based registration method. Statistical results of target-based registration are presented in Tables II and III.

Once all scans are registered together, the registration of epochs can be done. Here, we chose the C2C registration method on account of the fact that spherical targets were not put at the same place in the each of the epochs and they cannot be used anymore. The statistical results of registration are shown in the Table IV.

As it can be seen from Table IV, the alignment of all epochs resulted in overall error of 1.3 mm (for tower I) and 1.2 mm (for tower II), which means the average distance between two closest points. The registration errors are primarily caused by

TABLE IV
SCAN STATISTICS OF EPOCH I, EPOCH II, AND EPOCH III

| | Tower I | Tower II |
|---|---|---|
| Maximum point error, mm | 2.3 | 2.3 |
| Mean point error, mm | 1.3 | 1.2 |
| Minimum overlap, % | 56.5 | 65.2 |

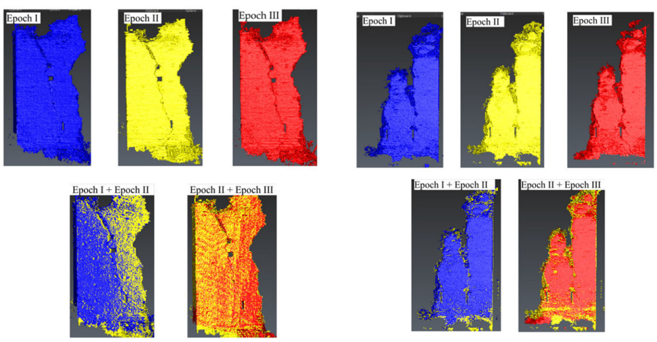


(a) (b)

Fig. 9. (a) Results of C2C registration of epochs of Tower I. (b) Results of C2C registration of epochs of Tower II. The first raw shows each of the epochs separately and the second raw shows the results of their alignment.

measurement errors, which can be reduced by fitting the appropriate scanning geometry. Another factor of the errors is the point spacing between the datasets in overlap area. Reducing the distance between TLS' positions and increasing the density of point clouds may significantly lower the registration errors. In practice, the minimum mm errors of epochs' registration are of vital importance for deformation monitoring. In our case, the obtained errors are relatively small and acceptable for the deformation monitoring of heritages. The final results after the C2C registration method are shown in Fig. 9(a) and (b).

The last step in data processing was point cloud filtering. Such obstructions as dust, strong wind, or passing vehicles may seriously affect the measurement and cause noise in data. Because the line of sight during the process of scanning was not impacted by any obstructions that listed above, there was no need to apply filters for noise removal, except for edge artifact filter which helps to eliminate artifacts at the edges of object. Since the object of interest was only the front wall of the Tower, it was not necessary to include all points in displacements computation (such as trees, grass, road, etc.) and all these extra points were removed from dataset. It was done by means of clipping box. Fig. 10(a) and (b) illustrates the process of deleting points. After that, the part of tower was saved in "e57" format and exported to the demo version of Cyclone 3DR software for further displacement analysis. Consequent steps in displacement analysis were performed in local coordinate system obtained after the registration of epochs.

## VI. RESULTS AND DISCUSSION

Displacement analysis was performed using demo version of Cyclone 3DR software by C2C method of distance computation. The results of analysis for the first and second periods are given

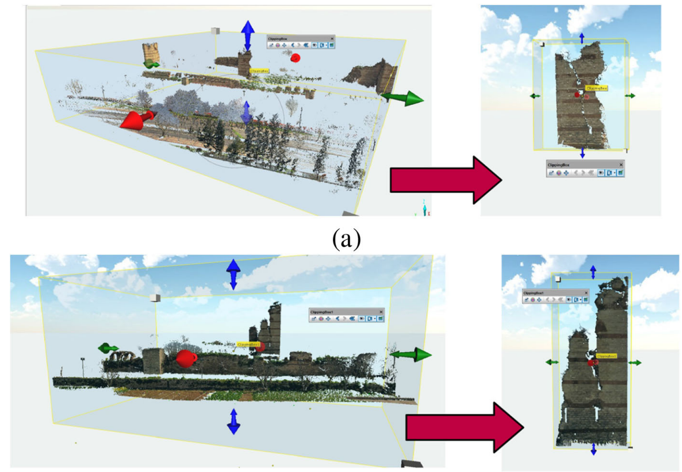

(a)

(b)

Fig. 10. (a) Point cloud filtering by means of clipping box of Tower I. (b) Point cloud filtering by means of clipping box of Tower II.

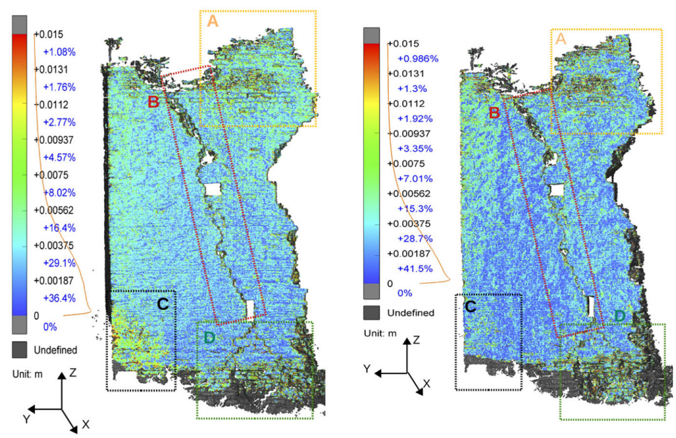


(a) (b)

Fig. 11. Deviation maps of tower I with areas of change highlighted (A, B, C, and D). (a) First period comparing. (b) Second period comparing.

in the form of colored maps. The color scale represents the values of 3-D displacements in meters. Grey patterns on the scale and on the map indicate areas that were not identified during the distance computation. The *Z*-axis represents a vertical direction. The *Y*-axis is oriented to the North and the *X*-axis is perpendicular to the *Y*-axis. All displacements have a positive value which means that the points of epoch II and epoch III are in front of those in the epoch I, which was selected as the reference frame.

The displacement map of tower I is given in Fig. 11(a) and (b) and the percentage distribution of deviations is shown in Fig. 12. The trend of the results illustrates that displacements occurred in the first period substantially higher in values, compared to the second period. Overall, the values ranged between 0 mm and 15 mm, with the average of 7 mm.

Fig. 13(a)–(d) shows the distribution of displacements in Sections A, B, C, and D. Displacements in highlighted sections in the first period are much higher compare to the displacements in the second period. Section A highlights its strong weathering

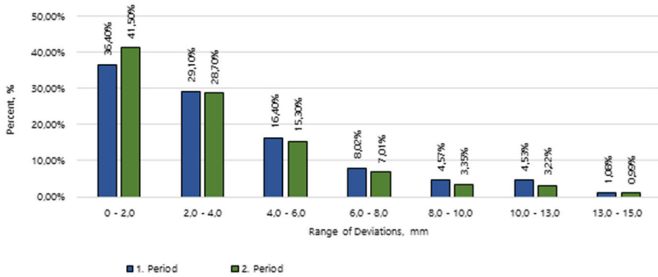


Fig. 12. Percentage distribution of deviations in cloud-to-cloud analysis of tower I.

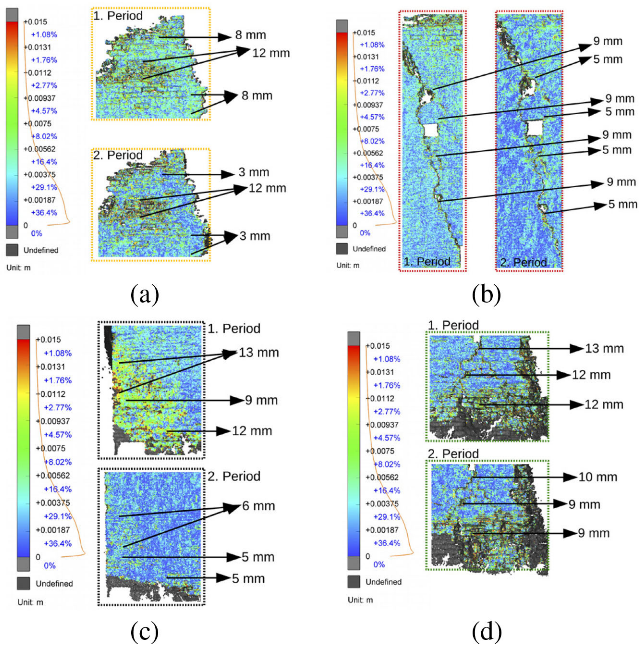


Fig. 13. Distribution of displacements in the highlighted areas of tower I. (a) Area A. (b) Area B. (c) Area C. (d) Area D.

susceptibility. It is unsurprisingly to find a considerable movement in the Sections B and D due to huge cracks. Alternatively, it could simply mean that these parts of the structure undergo deformations independently of earthquake and therefore, it is reasonable to expect the continuation of displacements. In the Section C, however, the obtained values of deviations are much lower in the second period compare to the first period. This may occurred due to construction weaknessess and Section C can be construed as zone with potential risk of damage. It is obvious that another earthquake may destroy this corner.

The results of displacement computation of the tower II is given in Fig. 14(a) and (b), and Fig. 15 shows the percentage distribution of deviations. The range of displacements is changed from 0 to 20 mm. From Fig. 14, key findings illustrate that entire surface of tower II underwent displacements in the ragne of 7–15 mm in the first period comparing, and 2–7 mm in the second period. These findings are expected, since in the first period an earthquake $M_W$ 5.7 occurred, while in the second period there was not any natural hazards.

Fig. 16(a)–(d) shows the distribution of displacements in Sections A, B, C, and D. Sections A and B have great structural

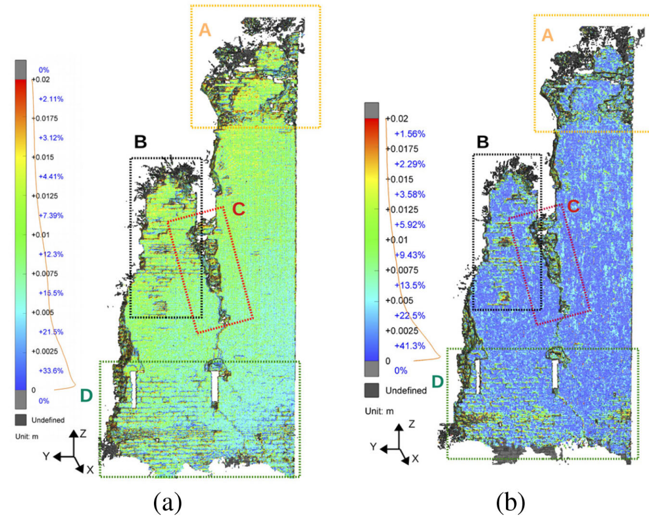


Fig. 14. Deviation map of tower II with areas of change highlighted (A, B, C, and D). (a) First period comparing. (b) Second period comparing.

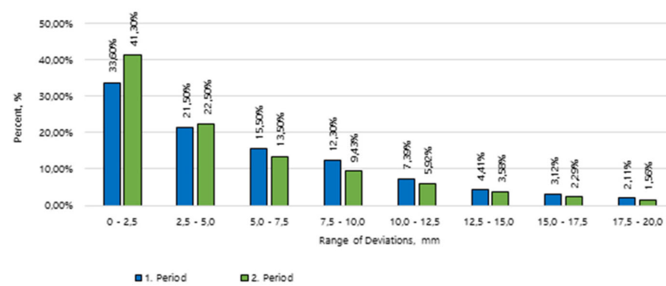


Fig. 15. Percentage distribution of deviations in cloud-to-cloud analysis of tower II.

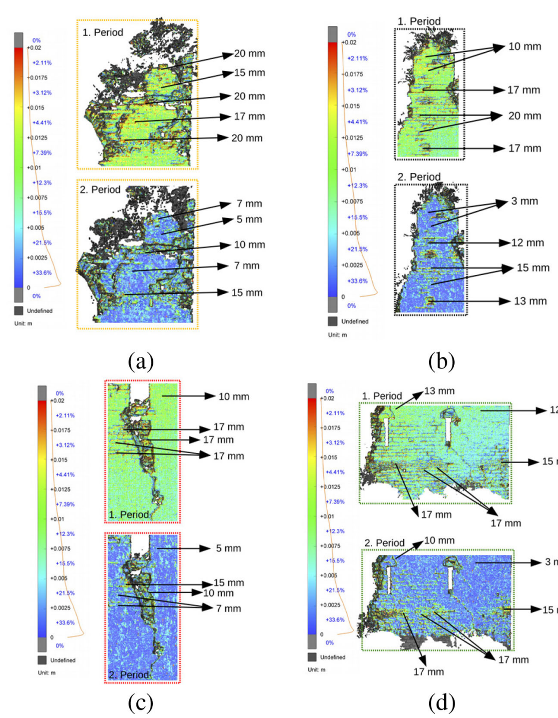


Fig. 16. Distribution of displacements in the highlighted areas of tower II. (a) Area A. (b) Area B. (c) Area C. (d) Area D.

weaknesses and their positions been unstable. The discontinuities in bricks alignments in Section D is been purely seen on the deviation maps.

## VII. Conclusion

In this article, we performed a geodetic monitoring of historical structure that was deformed because of earthquake with the magnitude of Mw 5.7. For this purpose, TLS technology was used, and this instrument showed itself as a good tool that allows for the dense point cloud acquisition and can provide an accurate realistic image of the scanned object. The displacement analysis is influenced by registration errors, thus, a good registration, preferably with an accuracy of a few mm is a main requirement for geodetic monitoring. Furthermore, the scanning geometry and the point cloud density must be also chosen on the appropriate level. Returning to the hypothesis posed at the beginning of this article, it is now possible to state that studied towers were exposed to displacements because of earthquake that struck approximately 60 km from the structure. The case study shows how TLS approach succeed in deformation monitoring of historical site, especially how TLS data can help to detect a zone of potential structural damage deriving deformations within the mm accuracy. The results from this article have two main significances. First, the conducted analysis gives insight on the assessment of building behavior to actions resulting from earthquake. Second, the results provide scientists with the opportunity to consider the critical state of Land Walls.

As a final conclusion, it can be said that proposed methodology can be applied not only to monitoring separate historical buildings, but also large structures such as damps or bridges with the final aim of risk prediction. We believe that our method could be used as guideline in the field of deformation monitoring and other kind of applications that deal with 3-D point cloud data.

## Acknowledgment

This project is the result of M.Sc. Thesis “Characterizing Deformation of Istanbul Wall by Geodetic Terrestrial Laser Scanner” submitted in Bogazici University, Istanbul, Turkey. The corresponding author would like to thank her Thesis advisors Prof. Dr. Haluk Ozener and Dr. Onur Yilmaz for their contributions. Also, the authors would like to thank Mr. Hasan Bal from FARO Turkey for his assistance and valuable advices during all work stages. Last but not least, the authors wish to thank Dr. Asli Sabuncu for her productive comments and proofreading during preparing this article.

## References

[1] V. Pagounis, O. Arabatzi, M. Tsakiri, and D. Tsini, “Geodetic technology for cultural heritage monitoring—The case study of Klepsydra at the acropolis of Athens,” in *Proc. 8th Intern., Symp. Conserv. Monuments Mediterranean Basic*, May 2010.

[2] S. Baselga, P. Garrigues, J. L. Berné, A. B. Anquela, and A. Martín, “Deformation monitoring in historic buildings: A case study,” *Surv. Rev.*, vol. 43, no. 323, pp. 484–492, 2011.

[3] A. Pellegrinelli, A. Furini, and P. Russo, “Earthquakes and ancient leaning towers: Geodetic monitoring of the bell tower of San Benedetto church in Ferrara (Italy),” *J. Cultural Heritage*, vol. 15, no. 6, pp. 687–691, 2014.

[4] B. Bhadrakom and K. Chaiyasarn, “As-built 3D modeling based on structure from motion for deformation assessment of historical buildings,” *Int. J. Geomate*, vol. 11, no. 24, pp. 2378–2384, 2016.

[5] S. L. Ullo, C. Zarro, K. Wojtowicz, G. Meoli, and M. Focareta, “LIDAR-based system and optical VHR data for building detection and mapping,” *Sensors*, vol. 20, no. 5, 2020, Art. no. 1285.

[6] A. Guarnieri, N. Milan, and A. Vettore, “Monitoring of complex structure for structural control using terrestrial laser scanning (TLS) and photogrammetry,” *Int. J. Architect. Heritage*, vol. 7, no. 1, pp. 54–67, 2013.

[7] P. Tang, F. Chen, X. Zhu, and W. Zhou, “Monitoring cultural heritage sites with advanced multi-temporal InSAR technique: The case study of the summer palace,” *Remote Sens.*, vol. 8, no. 5, 2016, Art. no. 432.

[8] D. Infante *et al.*, “Assessment of building behaviour in slow-moving landslide-affected areas through DInSAR data and structural analysis,” *Eng. Struct.*, vol. 199, 2019, Art. no. 109638.

[9] S. L. Ullo *et al.*, “Application of DInSAR technique to high coherence Sentinel-1 images for dam monitoring and result validation through *in situ* measurements,” *IEEE J. Sel. Top. Appl. Earth Observ. Remote Sens.*, vol. 12, no. 3, pp. 875–890, Mar. 2019.

[10] D. Infante *et al.*, “Monitoring of strategic buildings in civil protection activities via remote sensing data,” *IEEE Aerosp. Electron. Syst. Mag.*, vol. 34, no. 10, pp. 6–16, 2019.

[11] E. Bonali, A. Pesci, G. Casula, and E. Boschi, “Deformation of ancient buildings inferred by terrestrial laser scanning methodology: The Cantalovo church case study (Northern Italy),” *Archaeometry*, vol. 56, no. 4, pp. 703–716, 2014.

[12] G. Vacca, F. Mistretta, F. Stochino, and A. Dessi, “Terrestrial laser scanner for monitoring the deformations and the damages of buildings,” *Int. Arch. Photogramm., Remote Sens. Spatial Inf. Sci.*, vol. 41, no. B5, pp. 453–460, 2016.

[13] G. D. Georgopoulos, E. C. Telioni, and A. Tsontzou, “The contribution of laser scanning technology in the estimation of ancient greek monuments' deformations,” *Surv. Rev.*, vol. 48, no. 349, pp. 303–308, 2016.

[14] M. O. Selbesoglu, T. Bakirman, and O. Gokbayrak, “Deformation measurement using terrestrial laser scanner for cultural heritage,” *Int. Arch. Photogramm., Remote Sens. Spatial Inf. Sci.*, vol. 42, pp. 89–93, 2016.

[15] J. Guo, L. Yuan, and Q. Wang, “Time and cost analysis of geometric quality assessment of structural columns based on 3D terrestrial laser scanning,” *Automat. Construction*, vol. 110, 2020, Art. no. 103014.

[16] F. Mistretta, G. Sanna, F. Stochino, and G. Vacca, “Structure from motion point clouds for structural monitoring,” *Remote Sens.*, vol. 11, no. 16, 2019, Art. no. 1940.

[17] F. Uray, A. Metin, and A. Varlik, “3D architectural surveying of Diyarbakir wall's Ulu Beden tower with terrestrial laser scanner,” in *Proc. World Multidisciplinary Earth Sci. Symp.*, 2015, pp. 73–78.

[18] P. Redweik, J. J. de Sanjosé Blasco, M. Sánchez-Fernández, A. D. Atkinson, and L. F. Martínez Corrales, “Tower of Belém (Lisbon)–status quo 3D documentation and material origin determination,” *Sensors*, vol. 20, no. 8, 2020, Art. no. 2355.

[19] S. Al-Kheder, Y. Al-Shawabkeh, and N. Haala, “Developing a documentation system for desert palaces in Jordan using 3D laser scanning and digital photogrammetry,” *J. Archaeol. Sci.*, vol. 36, no. 2, pp. 537–546, 2009.

[20] D. S. Grant, “Cloud to cloud registration for 3D point data,” Open Access dissertations, 161, 2013. [Online]. Available at: https://docs.lib.purdue.edu/open_access_dissertations/161

[21] B. van Goor, “Change detection and deformation analysis using terrestrial laser scanning. Case study of the metro tunnel at rotterdam central station,” M.S. thesis, Geomatics Dept., Delft Univ. Technol., Delft, The Netherlands, 2011.

[22] S. Turnbull, *The Walls of Constantinople AD 324–1453*. London, U.K.: Bloomsbury Publishing, 2012.

[23] [Online]. Available: http://www.throneworld.com/oathofempire/geographica/constantinople.jpg

[24] O. E. Durusoy and M. C. Can, “Conservation of the land walls protection area by renewal (!): Evaluating the spatial effects of the law no. 5366 through “Zeytinburnu culture valley project” of Istanbul,” *Megaron*, vol. 13, no. 4, pp. 505–520, 2018.

[25] G. C. Ince, “Probabilistic seismic hazard assessment of the historical peninsula of Istanbul,” *Natural Hazards Earth Syst. Sci.*, vol. 12, no. 11, pp. 3483–3493, 2012.

[26] G. C. Ince, M. Yildirim, K. Özaydin, and P. T. Özener, “Seismic microzonation of the historic peninsula of Istanbul,” *Bull. Eng. Geol. Environ.*, vol. 67, no. 1, pp. 41–51, 2008.

[27] Ö. Undul and A. Tugrul, “The engineering geology of Istanbul, Turkey,” in *Proc. 10th IAEG Int. Congr.*, 2006, pp. 6–10.

[28] A. S. Krlangc, M. G. Kesti, M. Erdik, and E. Cakt, “Temporary earthquake retrofit of the land walls in Istanbul,” in *Proc. 14th Eur. Conf. Earthq. Eng.*, Aug./Sep. 2010.

[29] B. Bayram, G. Nemli, T. Ozkan, O. E. Oflaz, B. Kankotan, and I. Cetin, “Comparison of laser scanning and photogrammetry and their use for digital recording of cultural monument case study: Byzantine land walls-Istanbul,” in *Proc. ISPRS Ann. Photogramm., Remote Sens. Spatial Inf. Sci.*, 2015, vol. II-5/W3, pp. 17–24.

[30] G. C. Ince, “Geological and geotechnical structure of historical peninsula (Istanbul), and its seismic microzonation,” (in Turkish), in *Proc. 6th Nat. Conf. Earthq. Eng.*, Oct. 2007, pp. 163–172.

[31] F. Calo, S. Abdikan, T. Görüm, A. Pepe, H. Kiliç, and F. Balik Şanli, “The space-borne SBAS-DInSAR technique as a supporting tool for sustainable urban policies: The case of Istanbul megacity, Turkey,” *Remote Sens.*, vol. 7, no. 12, pp. 16519–16536, 2015.

[32] N. Lom, S. C. Ülgen, M. Sakinç, and A. C. Şengör, “Geology and stratigraphy of Istanbul region,” *Geodiversitas*, vol. 38, no. 2, pp. 175–195, 2016.

[33] M. Tekin *et al.*, “1:25.000 scaled geological map,” Municipal Council Istanbul, 2007.

[34] S. Ergintav *et al.*, “Istanbul’s earthquake hot spots: Geodetic constraints on strain accumulation along faults in the Marmara seismic gap,” *Geophys. Res. Lett.*, vol. 41, no. 16, pp. 5783–5788, 2014.

[35] A. O. Oncel and T. Wilson, “Evaluation of earthquake potential along the northern Anatolian fault zone in the Marmara sea using comparisons of GPS strain and seismotectonic parameters,” *Tectonophysics*, vol. 418, no. 3/4, pp. 205–218, 2006.

[36] N. Ambraseys, “The seismic activity of the Marmara sea region over the last 2000 years,” *Bull. Seismol. Soc. Amer.*, vol. 92, no. 1, pp. 1–18, 2002.

[37] N. N. Ambraseys and J. A. Jackson, “Seismicity of the sea of Marmara (Turkey) since 1500,” *Geophys. J. Int.*, vol. 141, no. 3, pp. F1–F6, 2000.

[38] KOERI, Bogazici University Kandilli Observatory and Earthquake Research Institute, Earthquake Catalogue, 2019. [Online]. Available at: http://www.koeri.boun.edu.tr/sismo/zeqdb/

[39] G. Hepyörük, “Investigation on the potential usage of terrestrial laser scanners in the 3D modelization and the documentation of historical and cultural assets and Karacabey Tomb model,” (in Turkish), Ph.D. dissertation, Geomatic Eng. Dept., Selçuk Univ., Konya, Türkiye, 2015.

[40] T. Temizer *et al.*, “3D documentation of a historical monument using terrestrial laser scanning case study: Byzantine water cistern, Istanbul,” in *Proc. Int. Arch. Photogramm., Remote Sens. Spatial Inf. Sci.*, 2013, Art. no. W2.

[41] *FARO Focus 330 HDR Manuals*, 2016. [Online]. Available: https://knowledge.faro.com/Hardware/3D_Scanners/Focus/User_Manuals_for_the_Focus3D_X_330_or_330_HDR

[42] J. I. San José Alonso, J. Martínez Rubio, J. J. Fernández Martín, and J. G. Fernández, “Comparing time-of-flight and phase-shift. The survey of the royal pantheon in the Basilica of San Isidoro (León),” in *Proc. Int. Arch. Photogramm. Remote Sens. Spatial Inf. Sci.*, 2011, pp. 377–385.

[43] C. Suchocki, “Comparison of time-of-flight and phase-shift TLS intensity data for the diagnostics measurements of buildings,” *Materials*, vol. 13, no. 2, 2010, Art. no. 353.

[44] V. E. Oniga and C. Chirila, “Hausdorff distance for the differences calculation between 3D surfaces,” *J. Geodesy Cadastre RevCAD*, vol. 15, pp. 193–202, 2013.

[45] B. M. Jafari, “Deflection measurement through 3D point cloud analysis,” M.S. thesis, Dept. Civil and Infrastructure Eng., George Mason Univ., Fairfax, VA, USA, 2017.

[46] P. Minetola, L. Iuliano, and F. Calignano, “A customer-oriented methodology for reverse engineering software selection in the computer aided inspection scenario,” *Comput. Ind.*, vol. 67, pp. 54–71, 2015.

[47] M. V. Özdogan and A. H Deliormanli, “Determination of deformations occurred in underground drift by terrestrial laser scanner,” (in Turkish), *Dokuz Eylul Universitesi Muhendislik Fakultesi Fen ve Muhendislik Dergisi*, vol. 20, no. 59, pp. 663–675, 2018.

[48] A. Costa, J. M. Macias Solé, J. M. Puche, and I. Fontanilles, “Structural deformations of the Visigotic church of Sant Miquel de Terrassa,” (in Spanish), *Informes de la Construcción*, vol. 71, 2019, Art. no. 555.

[49] T. Ercan, “The use of laser scanning in civil and earthquake engineering,” M.S. thesis, Earthquake Eng. Dept., Bogazici Univ., Istanbul, Turkey, 2017.

**Maryna Batur** was born in Dnipro, Ukraine, in 1987. She received the B.S. degree in mine engineering from the National Mining University of Ukraine, Dnipro, Ukraine, and the graduate degree in geodesy from Bogazici University, Istanbul, Turkey, in 2008 and 2020, respectively.

From 2008 to 2012, she was a Research Assistant with the Institute of Geotechnical Mechanics, National Academy of Science of Ukraine, Dnipro, Ukraine. She is currently with the Department of Geodesy, Kandilli Observatory and Earthquake Research Institute, Bogazici University, Istanbul, Turkey, working on the Scientific Project “Use of Terrestrial Laser Scanning Technology in Architect Documentation” and planning to continue her study in the Ph.D. degree. Her research interests include terrestrial laser scanning technology, deformation measurements, and analysis of historical structures.

Ms. Batur was the recipient of the Grant of the President of Ukraine for the Research Project, in 2010 and was also the recipient of the scholarship of the President of Ukraine for Significant Achievements in the Field of Technical Science, in 2012.

**Onur Yilmaz** received the graduate degree in geodesy and photogrammetry engineering from Yildiz Technical University, Istanbul, Turkey, in 1990, and the Ph.D. degree in geodesy from Bogazici University, Istanbul, Turkey, in 2000.

He has been working with Kandilli Observatory and Earthquake Research Institute, Bogazici University, Istanbul, Turkey, since 1991, started as Research Assistant and currently as an Instructor. He is involved in numerous interdisciplinary earthquake and GNSS related research projects. His research interests include deformation, GNSS, TLS, and gravity.

**Haluk Ozener** received the B.S. degree in geodesy and photogrammetry engineering from Istanbul Technical University, Istanbul, Turkey, in 1988, and the M.Sc. degree in stochastic models of local horizontal networks for geodynamic problems and Ph.D. degree in monitoring regional horizontal crustal movements by individual microgeodetic networks established along plate boundaries from Bogazici University, Istanbul, Turkey, in 1992 and 2000, respectively.

He is currently a Director with Kandilli Observatory and Earthquake Research Institute, Bogazici University and a Chair with the Geodesy Department. He has authored/coauthored more than 40 research articles in international journals and his papers have been cited over 1880 times according to the records of Web of Science (without self-citations). Participating in more than 50 International and National academic research projects (e.g., FP7 and Horizon 2020) as a PI, Consultant, and Researcher, he has scientifically contributed more than 350 scientific publications (indexed by SCI, SCI-Expanded, research reports, conference papers, etc.) either as the first author or coauthor. As an organizer, moderator, or scientific committee member, he has participated in more than 60 International and National Scientific meetings. His research interests include geodesy, GPS, geodynamics, earthquake hazards, crustal and surface deformation, stochastic modeling and establishment of geodeticn, and project management.

Prof. Ozener served as the Chairman of the Tectonic and Earthquake Geodesy Commission under the International Association of Geodesy and Chairman of the International WEGENER Working Group. He is still serving as the President of the Earthquake Association, representative of the universities in Turkish National Geodesy Commission, Chairman of the International Relations Commission of the Turkish Chamber of Survey and Cadastre Engineers. He has been a member of the Disaster and Emergency Advisory Board of Ministry of Interior, since 2015.